Toxicity of zinc oxide and iron oxide engineered nanoparticles to *Bacillus subtilis* in river water systems

Samuel K. Learenga, Eunice Ubomba-Jaswab, Ndeke Musee[a,*]

[a]Emerging Contaminants Ecological and Risk Assessment (ECERA) Group, Department of Chemical Engineering, University of Pretoria, Private Bag X20, Hatfield 0028, Pretoria, South Africa

[b]Water Research Commission, Pretoria, South Africa

Abstract

Zinc oxide (nZnO) and iron oxide ($nFeO_x$) engineered nanoparticles (ENPs) are widely used in consumer products and industrial applications, and consequently, are continuously being emitted into the environment. Numerous studies have reported on the toxicity of ENPs to bacteria, especially in synthetic aqueous exposure media. However, investigations in natural aqueous exposure media such as river water are limited. Herein, the toxicity of nZnO and maghemite iron oxide (γ-nFe_2O_3) on *Bacillus subtilis* was investigated in two natural river water samples; the Elands river (ER) and Bloubank river (BR). Four endpoints, namely; cell viability, cell membrane integrity, adenosine triphosphate levels (ATP), and reactive oxygen species (ROS) production were evaluated to determine the effects of the ENPs on bacteria. nZnO induced significant reduction in cell viability and membrane integrity at higher tested concentrations of 100 and 1000 $\mu g\ L^{-1}$ in ER; but none were observed in BR. In addition, higher decrease in ATP levels were observed in ER than in BR, and ROS production was negligible irrespective of ENPs type and exposure media. The γ-nFe_2O_3 induced no effects on *B. subtilis* on all tested endpoints. These results demonstrated that the observed differences in effects of nZnO towards *B. subtilis* were influenced by the physicochemical properties of each river water. Therefore, the unique physicochemical properties of natural aqueous media were established to be key determinant attributes in enhancing or inhibiting the effects of ENPs to bacteria.

*Corresponding author: Ndeke Musee; Email: Ndeke.musee@up.ac.za; museen2012@gmail.com

Environmental Significance

Increasing zinc oxide (nZnO) and iron oxide ($nFeO_x$) engineered nanoparticles global production and associated uses are likely to increase their presence, for example, in freshwater systems. Thus, assessment of likely environmental impacts of ENPs are critical; although to date very limited studies have investigated their effects on microorganisms under relevant environmental exposure-media and –concentration(s) scenarios. Herein, effects of nZnO and γ-nFe_2O_3 on *Bacillus subtilis* were assessed in natural water media using multiple endpoints with variant degrees of toxicity sensitivities to contaminants. Toxicity of nZnO was shown to be dependent on water physicochemical properties, however; the same properties were observed to mitigate likely γ-nFe_2O_3–cell interactions. Findings on sub-lethal endpoints like ATP production revealed nanoparticle toxicity unlike traditional endpoints such as cell viability where no bacterial effects were observed. Our study contributes towards understanding of plausible nanoparticle-organism interaction mechanisms in natural water matrices, necessary for prediction of meaningful environmental outcomes.

Introduction

Increasingly, numerous consumer products have incorporated engineered nanoparticles (ENPs) in recent years[1-5] due to their unique physicochemical properties to enhance functionality and meet consumer needs. Among the most produced and used top five ENPs in the fast-growing nanotechnology market are zinc oxide (nZnO) and iron oxide ($nFeO_x$)[6, 7]; with medium-term production growth expected to increase.[8] For example, nZnO are widely incorporated in consumer products, e.g. cosmetics, sunscreens, nanomedicine, paints and coatings due to their UV radiation blocking properties[9, 10]; whereas linked to their superior properties and functionalities (e.g. magnetic, catalytic, etc.) γ-nFe_2O_3 are used in biomedical imaging, environmental remediation catalysis, fertilizers, pigments, sensors, bio-medical and lithium ion batteries.[11-14] Therefore, as the use and applications of both ENPs become more common, their release and eventual accumulation into the environment continue to grow exponentially.[6, 15, 16] As a result, this exponential growth will likely surpass current predicted concentration of iron oxides and nZnO concentrations predicted at 12.8 to 44 ng L^{-1} [17], and 2 to 360 ng L^{-1} [18-20] in Europe, respectively, for example.

The antimicrobial properties of ENPs heighten their likelihood to exert adverse impacts to non-target and useful microbes once in the aquatic systems[10, 15, 21], for example, *Sinorhizobium meliloti*[22] and *Shewanella oneidensis*[23], respectively, essential for nitrogen fixation and metal reducing capacity. To date, observed ENPs toxicity to microbes have been attributed to oxidative stress through generation of reactive oxygen species (ROS), release of toxic metallic ions, surface contact, cell membrane damage, and internalization of ENPs particulates.[10, 21, 24, 25] Both the interaction of ENPs and microorganisms as well as their concomitant toxicity are dependent on inherent ENPs physicochemical properties and water chemistry.[5, 26-28] In particular, numerous studies have demonstrated the influence of water chemistry (e.g. pH, ionic strength (IS), light, and natural organic matter (NOM)) [29, 30] on ENPs transformation, and the eventual observed toxicity to bacteria.[31, 32]

Notably, most of these studies investigated the influence of water chemistry on ENPs transformation and observed toxicity predominantly in synthetic media although such media are too simplistic to accurately represent the actual complex aquatic ecosystems.[33, 34] This is because of the complexities and high variability of freshwater systems that can alter the transformation of ENPs[35-37], and in turn, yield different toxicological outcomes, for example, to microbes.[31, 38] Thus, data and information on the effects of ENPs to microbes in these deterministic freshwater systems remain scarce, and therefore, impedes realistic assessment of ENPs risks to the environment.

To date, experimental toxicity investigations of ENPs have been assessed at concentrations several magnitudes above both modelled and measured ENPs concentrations,[39-41] consequently, this has severely limited our ability to realistically assess their likely implications to the aquatic systems. Only few studies, for instance, have demonstrated the effects of ENPs on bacteria at concentrations within an order of magnitude to those predicted or measured in actual environmental matrices. Yi and Cheng[28] evaluated the effects of nAg on *Bacillus subtilis* in natural waters whilst Wilke et al[42] examined the effects of Ag and TiO_2 on *Escherichia coli*. Studies from the Gray's group[43, 44] have also demonstrated the importance of using toxicity measures like adenosine triphosphate (ATP) depletion to determine the effects of ENPs on microorganisms to obtain a complete understanding of the likely risks posed by ENPs in the environment, even at very low concentrations where cell

death is not apparent. Even in dark conditions, for example, at concentrations < 250 μg L^{-1}, the obtained results demonstrated that bacterial ATP levels can be significantly reduced by nAg and nZnO[42, 44] with likely adverse implications to the environment.

The highlighted knowledge gaps raise the need to understand the implications of ENPs in the aquatic systems, particularly at environmentally relevant concentrations. Therefore, in this work the toxicological effects of the nZnO and γ-nFe_2O_3 on *B. subtilis* as influenced by water chemistry characteristics were evaluated. Here, the natural water chemistry matrix differences were due to their distinctive sources (two river water systems). *B. subtilis*, an environmentally ubiquitous organism was selected as the model organism due to its ability to tolerate extreme environmental conditions and stress.[28, 45] Secondly, the organism has been used in nanotoxicity studies, and is reported to be more sensitive to ENPs compared to gram-negative bacteria e.g. *E. coli*, or other gram-positive bacteria like *Streptococcus aureus*.[46] Understanding the induced toxicity of ENPs on microorganisms in natural water by investigating four end-points: cell viability, membrane integrity, ATP levels, and oxidative stress from ROS can aid to better assess their risk to natural water matrices such as river water used in this study.

Experimental procedure

Freshwater sampling

The freshwater samples were collected from two rivers, namely; the Elands river (ER) (25°32'58.4"S 28°33'53.4"E, Gauteng Province, South Africa) and Bloubank river (BR) (26°01'20.3"S 27°26'31.6"E, North West Province, South Africa). The collected water samples (from ER and BR) were used as exposure matrixes to represent different complex environmental surface freshwater chemistries. The collected river water was filtered using Whatman No. 1 filter paper (pore size: 11 μm) followed by filtration through 0.2 μm pore sized membrane filters to remove microorganisms and larger particles. All water samples were stored at 4°C until analysis. The physicochemical properties of both river water systems are summarised in Table 1.

Materials

nZnO (< 100 nm, 20% dispersion in H_2O, CAS 1314-13-2), nFe_2O_3 (γ- Fe_2O_3, < 50 nm, nano powder, CAS 1309-37-1), 2′,7′-Dichlorofluorescin diacetate (DCF-DA) and Dimethyl sulfoxide (DMSO) were purchased from Sigma-Aldrich, South Africa. According to the manufacturer, the particle sizes were < 100 nm and < 50 nm for nZnO and nFe_2O_3, respectively. All chemicals were analytical grade reagents and used as received without further purification. The *Bacillus subtilis* (ATCC 11774) strain was purchased from Anatech (Johannesburg, South Africa).

Table 1: Physicochemical parameters of freshwater samples from Bloubank and Elands River

Parameter	Unit	Bloubank River (BR) water	Elands River (ER) water
pH		7.9	8.1
DOC[a]	mg C L^{-1}	8.25	5.51
Electrical conductivity	ms/m 25°C	39.8	19.6
COD[b]	mgL^{-1}	21.3	6.67
Alkalinity	mgL^{-1}	217	75.6
NH_4^+	mgL^{-1}	3.4	4.27
NO_3^-	mgL^{-1}	0.2	0.33
Cl^-	mgL^{-1}	12.9	17.1
SO_4^{2-}	mgL^{-1}	6.77	9.03
PO_4	mgL^{-1}	1.23	0.57
Fe^{3+}	mgL^{-1}	<0.004	<0.004
Zn^{2+}	mgL^{-1}	0.01	0.008
Ca^{2+}	mgL^{-1}	36	14
Mg^{2+}	mgL^{-1}	31	9.82
Na^+	mgL^{-1}	22.4	15.6
K^+	mgL^{-1}	3.13	4.24
IS[c]	mM	5.23	2.43

[a]Dissolved organic matter; [b] Chemical oxygen demand; [c]Ionic strength - calculated by visual Minteq (Version 3.1)

Characterization of ENPs

The ENPs size and morphology were characterised by transmission electron microscope (TEM) (JEM 2010F, JEOL Ltd., Japan); with ENPs diameter measured using imageJ software (National Institutes of Health, USA) based on particle size analysis from several micrographs. Phase composition was determined using Bruker D8 Advance powder X-ray diffractometer (XPRD) with monochromatized Cu Kα radiation of wavelength (λ) 1.54 Å. The hydrodynamic diameter (HDD) and zeta potential (ζ-potential) for ENPs suspensions in river water were characterised using dynamic light scattering (DLS) on a Zetasizer Nano-ZS instrument (Malvern Instruments, UK), and results are listed in Table S1 (supporting information). Concentrations of 20 mg L^{-1} ZnO and 5 mgL^{-1} γ-nFe_2O_3 were used for hydrodynamic size and ζ-potential measurements.

To determine the dissolved metal concentrations of nZnO and γ-nFe_2O_3, suspensions of ENPs were prepared similarly to experimental conditions (bacterial culture and exposure preparation), without the bacteria. Nanoparticle suspensions were filtered through regenerated cellulose centrifugal filters with a 3 kDa molecular weight cut-off (Merck Millipore, Darmstadt, Germany) by centrifuging for 30 min at 4000 xg (Eppendorf 5810 R, Eppendorf, Germany), to remove undissolved ENPs, but allow dissolved ions in the aqueous phase to pass. The dissolved fraction was acidified with 5 µL of concentrated HNO_3 and the concentration of dissolved ions in the supernatant were analysed by inductively coupled plasma mass spectrometer (ICP-MS) (ICPE-9820, Shimadzu, Japan).

Visual MINTEQ (Version 3.1, https://vminteq.lwr.kth.se) was used to predict speciation of zinc in ER and BR water based on parameters listed in Table 1. The Stockholm Humic Model (SHM) was used with default parameters as model inputs.

Bacterial culture and exposure preparation

Bacterial strain *B. subtilis* was plated on sterilized lysogeny broth (LB) agar plates and stored at 4°C until use. For cell viability studies, a single colony was inoculated in LB broth and incubated at 30°C with shaking at 150 rpm overnight until cells attained mid-exponential phase (0.4 – 0.5 at OD_{600nm}). Bacterial cells were harvested by centrifugation at 7 500 xg for 5 min, washed once with physiological saline (0.85 % NaCl), and then once using filtered river water. The cells were finally re-suspended in filtered river water and final concentration of

cells used in the exposure tests adjusted to 2 x 10^8 CFU/mL (≈ 0.3 at OD_{600nm}) measured by direct plating counting.

Stock solutions of ENPs at concentration of 100 mg L^{-1} were prepared using ultrapure water (18 MΩ cm resistivity, Elga PureLab Option System, United Kingdom), and sonicated for 20 min using ultrasonic bath prior to exposure experiments. The stock suspensions were diluted to target nominal concentrations of, 10, 100 and 1000 μg L^{-1} for nZnO; and, 10, 100, 1000 and 10 000 μg L^{-1} for γ-nFe_2O_3 in 250 mL flasks containing bacterial cells (OD_{600nm} of 0.3) and river water to achieve a final volume of 25 mL. The controls were run without ENP suspensions. The flasks were incubated at room temperature (20 –23°C) on a rotating shaker at 75 rpm for 2 h under visible light (338 lux).

Cell viability and membrane integrity

Both exposed and non-exposed (control) samples were serially diluted in 0.85% NaCl, and thereafter, viable bacteria were determined on LB agar plate following the drop count method[47]. Nine drops of 20 μL for each dilution were transferred onto solid LB agar plates. The plates were incubated overnight at 37°C. The bacterial viability following exposure to ENPs suspensions was measured by counting the number of colony forming units (CFU) from the appropriate dilution on nutrient agar plates. Hence, the percentage of viable cells was determined by comparing the CFU per mL of the culture as a ratio of the number of CFU from ENPs exposed samples to non-exposed (control) samples. All viability experiments were done in triplicates and repeated twice.

The Live/Dead BacLight kit (Molecular Probes, US) was used to test the cell membrane integrity of bacteria following exposure to ENPs. Hundred-μL of ENPs exposed and non-exposed (control) samples were transferred to individual wells in a 96-well microplate (Greiner Bio-One, Austria), combined with 100 μL of SYT09/PI mixture (10/60 μM), and then mixed thoroughly. The PI and SYTO9 stain nucleic acids were used to differentiate between intact cells (live organisms–stained in green) and damaged cells (dead organisms – stained in red), respectively. The microplate was then incubated with assay reagents for 15 min at

room temperature (20–23°C) in the dark (covered by aluminium foil). Fluorescence was measured with excitation and emission wavelengths for SYTO9 and PI of 485/538 nm (green) and 485/635 (red), respectively, using a Flouroscan Ascent FL microplate reader (ThermoFisher, USA). A calibration curve was obtained using cells with known percentages of intact cells. For each test, three replicates of each treatment were included per plate, and two plates were used to ensure reproducibility.

Oxidative stress from ROS

Intracellular ROS following exposure to ENPs in the river water was determined as a measure of oxidative stress using the membrane permeable non-fluorescent dye 2′, 7′-dichlorofluorescin diacetate (DCF-DA, Sigma Aldrich). DCF-DA is converted into the fluorescent 2′, 7′-Dichlorofluorescin (DCF) after reacting with ROS, thus making the cell to fluoresce. Following the 2 h exposure, 150 μL of the exposed and non-exposed samples were transferred to 96-well microplates and incubated with DCF-DA (100 μM final concentration) for 30 min at 37°C under dark conditions (covered using aluminium foil). DCF fluorescence intensity was measured with a Flouroscan Ascent FL microplate reader (ThermoFisher, USA) at an excitation and emission wavelengths of 485 and 538 nm, respectively, to quantify ROS activity both in the treated and control groups. ENPs without bacteria were also incubated with DCF-DA as controls. ROS production was expressed as percentage fluorescence of the control over the exposed samples. For each test, three replicates of each treatment were added per plate, and two plates were used to ensure reproducibility.

Bacterial ATP levels

BacTiter-Glo Microbial Cell Viability assay (Promega, Germany) was used to quantify bacterial ATP levels. This was achieved by measuring luminescence signal intensity from reaction of luciferin and ATP to test bacterial activity changes in response to ENPs treatment. Hundred-μL of ENPs exposed and non- exposed samples were transferred to individual wells in a 96-well microplate combined with 100 μL of the BacTiter-Glo reagent and mixed thoroughly. The microplate was then incubated for 5 min at room temperature (20–23°C) under dark conditions (covered with aluminium foil). The luminescence signal

was measured using the Flouroskan Ascent FL microplate reader, and the results were expressed as relative percentage of ATP of exposed bacteria to the control. For each test, three replicates were included in each treatment per plate, and two independent microplates were used to ensure reproducibility of the results. Also, the potential interference of the ENPs with the BacTiter-Glo assay reagent were analysed to ascertain whether the effects observed were wholly due to ENPs treatment.

Statistical analysis

Data herein are expressed as mean with corresponding standard deviation (SD). Two-way analysis of variance (ANOVA) was used to evaluate statistical differences followed by *post hoc* Tukey's multiple comparisons tests. Differences between samples were considered statistically significant when at $p < 0.05$. All analyses were done with GraphPad Prism V7.04 (GraphPad Prism software Inc., San Diego, CA, USA).

Results and discussion

Nanoparticles characterization

The γ-nFe_2O_3 had a hexagonal shape and an average particle size of 41 ± 25 nm. nZnO exhibited non-uniform shapes consisting of hepta-, penta-, hexa-gonal, and rod shapes, with diameter ranging from 15 to 57 nm due to asymmetry of the morphology. The representative TEM images of the ENPs are shown in Fig. S1 a, b, e and f. Results from XRD revealed the crystalline phase of nZnO was zincite (Fig. S1 c) whereas that of nFe_2O_3 was maghemite (γ-nFe_2O_3) (Fig. S1 d). The ζ-potential for both ENPs were negative in all river water samples (Table S1), and at narrow range between -12.3 ± 0.6 and -15.1 ± 1.3 mV.

Zetasizer results indicated immediate aggregation of nZnO and nFe_2O_3 in both river water samples post-sonication (Table S1). nZnO had average sizes of 512 ± 22 and 1 069 ± 187 nm in ER and BR, respectively, whereas nFe_2O_3 had HDD of 958 ± 188 nm and 1 056 ± 120 nm in ER and BR, respectively (Table S1). High aggregation of ENPs observed in both river water samples was associated with low ζ-potential of between -12.3 ± 0.6 and -15.1 ±1.3 mV; considered to be too low as ζ-potential of above ± 30 mV is required to maintain ENPs

dispersed by charge stabilization[48], or against aggregation, or dispersion[49-51]. For both ENPs, increased aggregation was more significant in BR compared to ER after 2h (Table S1).

Figure S2 summarizes dissolution results of nZnO in both river water samples. Fe ions could not be detected as their concentration were below analytical detection limit. Indeed, nFe_2O_3 are known to exhibit very low or no dissolution in aqueous matrices[15, 52]. Dissolution of nZnO was observed to be concentration-dependent in similar fashion to earlier studies[31, 53-55]. At nominal exposure concentration of 100 μg L^{-1}, 14 μg L^{-1} of dissolved zinc were measured in ER compared to less than 2 μg L^{-1} in BR. At higher nominal exposure concentration of 1000 μg L^{-1}, higher dissolution of nZnO was observed in ER and BR water at values of 366 and 183 μg L^{-1}, respectively.

The observed differences in aggregation and dissolution in ER and BR were attributed to differences in water physicochemical properties (Table 1); which are known to influence the transformation processes of ENPs in aqueous matrices.[30, 35, 36] Natural organic matter (NOM) coating on ENPs in aquatic systems can either enhance or inhibit their aggregation and stability through mechanisms like electrostatic interaction and ligand exchange, among others. [56-59] Moreover, it has been reported that under high IS conditions and in the presence of NOM, likely cation binding enhances the aggregation of ENPs.[30, 57, 60]

In this study, aggregation of both ENPs was observed, with larger aggregate sizes in BR. This may be due to higher NOM content in BR (Table 1) that could have resulted in adsorption onto ENPs surfaces, likely through ligand exchange since both ENPs were negatively charged in both water samples. This is because NOM is known to strongly adsorb due to ligand exchange between carboxyl and hydroxyl groups of NOM, and the hydroxyl groups on ENPs.[30] Both river water samples had high NOM content (> 5 mg L^{-1}) which is within reported range of 0.1 to 30 mg L^{-1} in surface water[59, 61, 62], and therefore, rendered NOM dependent aggregation highly likely. [30, 59]

Secondly, differences in IS with both monovalent and divalent ions being higher in BR compared to ER (Table 1), could also explain the enhanced aggregation in the former, as such conditions are known to increase NOM and ENP complexes.[59, 63-65] Increased aggregation in BR were also linked to higher concentration of electrolytes (mainly divalent

ions e.g. Ca^{2+}, Mg^{2+}, etc.) via compression of the electric double layer (EDL) through the reduction of electrostatic repulsion between particles and/or formation of aggregates by cation bridging.[30, 66 55, 63, 64, 67] Consequently, nZnO dissolution in BR was significantly lower due to reduced surface area as larger aggregates were formed compared to those in ER water samples. Dissolved zinc from nZnO could have also been reduced due to complexation with NOM and PO_4, resulting to lesser concentration of ions measured in BR water. Li et al[31] and Lv et al[68] showed that release of Zn^{2+} decreased with increasing concentrations of PO_4 due to strong metal-complexation between the phosphates and metal ions. In this study, BR water had higher concentration of PO_4 than ER water, pointing to reduced bioavailability of the ions in the former.

The observed differences in the dissolution of nZnO were therefore linked to differences in aggregation and water chemistry component differences observed between ER and BR water samples. Similarly, results of Odzak et al[36] indicated enhanced aggregation and low dissolution of nZnO in freshwaters sourced from river and lake waters with high IS ranging between 3.4 and 6.4 mM compared with those characterized by low IS. These researchers' results are consistent with findings reported herein where in BR water samples with high IS of 5.23 mM had higher aggregation and low dissolution of nZnO when compared to low aggregation and high dissolution observed in ER with low IS of 2.43 mM.

Overall, results therefore point to NOM coating-controlled release of ions from ENPs in freshwater due to the blockage of active sites – which in turn – inhibits the diffusion of ions from ENPs surfaces; thus accounting for high aggregation and low dissolution observed in BR water samples characterised by both high NOM, and IS. In addition, complexation of metal ions with NOM and phosphates could also account for reduced dissolution of nZnO. These outlined transformations have direct or indirect influence on the bioavailability and toxicity of nZnO and γ-nFe_2O_3 in the two freshwater systems as discussed in the following sections.

Cell viability and membrane integrity

Results of *B. subtilis* exposure to nZnO and γ-nFe_2O_3 in ER and BR revealed distinctive cytotoxic effects (Fig. 1a and b). At higher concentrations of 100 and 1000 $\mu g\ L^{-1}$, nZnO

reduced *B. subtilis* viability in ER with markedly significant effects observed at 1000 μg L^{-1} ($p \leq 0.001$); whereas at 10 μg L^{-1} nZnO no viability inhibition was apparent. Conversely, exposure to nZnO in BR had no effect on cell viability at all tested concentrations (Fig. 1a) which was linked to larger aggregates formed in BR water samples as discussed in nanoparticles characterization section. This is because larger aggregates could not compromise cell integrity due to limited or lack of contact with cells. For the γ-nFe_2O_3, irrespective of the exposure concentration (10 – 10 000 μg L^{-1}) no effect on cell viability were observed in both water samples (Fig. 1b).

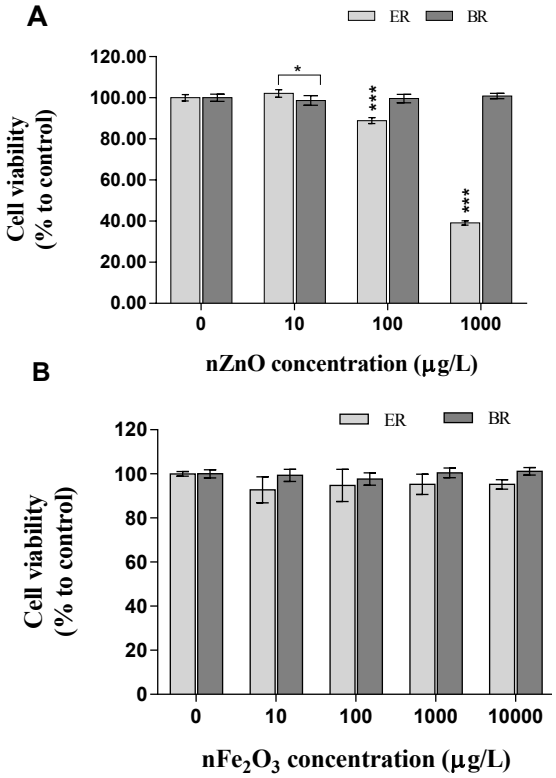

Fig. 1 Effects of (a) nZnO and (b) γ-nFe_2O_3 on *B. subtilis* viability in river water. Data represents the average ± SD (n=3). Asterisks (*) represent significance levels from Tukey's *post hoc* tests in two-way ANOVA (*$p < 0.05$, **$p \leq 0.01$, ***$p \leq 0.001$).

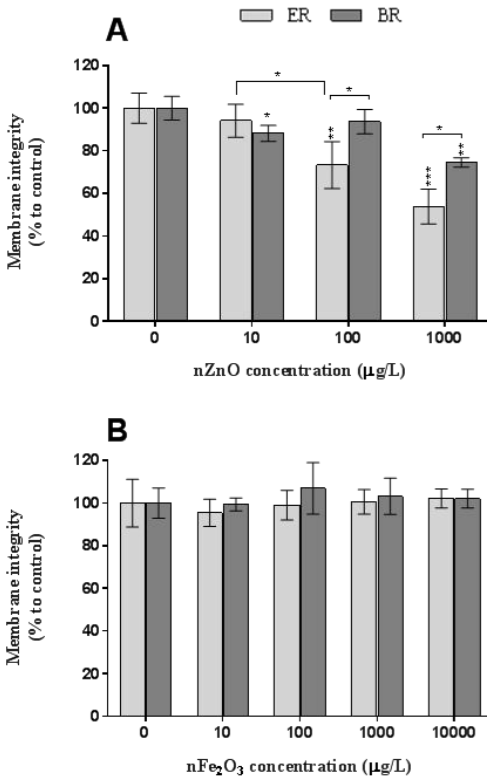

Fig. 2 Effects of (a) nZnO and (b) γ-nFe_2O_3 against *B. subtilis* cell membrane integrity in natural water. Data represents the average ± SD (n=3). Asterisks (*) represent significance levels from Tukey's *post hoc* tests in two-way ANOVA (*$p < 0.05$, **$p \leq 0.01$, *** ≤ 0.001).

Bacterial cell membrane integrity was also evaluated for both ENPs, and the results are summarized in Fig. 2. Effects of nZnO on cell membrane integrity were found to be concentration dependent in both river waters. For instance, results indicated that nZnO induced significantly higher effects on cell membrane integrity disruption at all concentrations in ER with maximum reduction of 46% (Fig. 2a), and the trend was similar to reduction in cell viability (61%) observed at the same concentration (Fig. 1a). A 26% cell membrane integrity disruption was observed in BR at 1 000 μg L^{-1}, but insignificant minimal effects at lower concentrations (Fig. 2a). Moreover, the cell membrane integrity significantly decreased ($p \leq 0.01$) in BR (1 000 μg L^{-1}) for nZnO, and the results were similar to those of 100 μg L^{-1} in ER (Fig. 2a). The observed differences on cell membrane integrity were attributed to two factors: (i) water physicochemical properties (Table S1) where in ER a marked reduction was observed, likely due to low aggregation and high dissolution of ENPs

(specifically nZnO), and (ii) the type of ENPs with nZnO inducing a higher disruption compared to that of γ-nFe_2O_3 (Fig. 2).

To date, the toxic effects of nZnO on bacteria have been widely reported, with effects linked to mechanisms such as nanoparticles surface contact and uptake, release of ions (Zn^{2+}), and ROS production.[31, 46, 69-74] In this study, the three mechanisms were evaluated in an effort to account for the observed cytotoxic effects of both ENPs on *B. subtilis*, and the results are discussed in the following paragraphs and sections. Concentration-dependent effects on cell membrane integrity were observed in both water samples (Fig. 2a) but cell viability effects were only observed in ER water samples (Fig. 1a). Our findings are consistent with other studies[71 53] where bacterial viability was found to be dependent on nZnO exposure dosage (2 ug L^{-1} to 5000 mg L^{-1}). Herein, the observed effects were linked to the increased dissolved zinc ions concentrations as the exposure concentration increased (Fig S2), which was dependent on the river water chemistry (Table 1). This is consistent with earlier findings where dissolved zinc from nZnO was established to be responsible for the observed toxicity to bacteria as influenced by exposure media chemistry.[31, 53] Herein, the effects of nZnO in ER may be linked to measured dissolved zinc of 366 ugL^{-1} compared to 183 ugL^{-1} in BR at nominal exposure concentration of 1 mgL^{-1}. Modelled speciation results of dissolved zinc species in both river water systems using visual Minteq showed that about 50% of dissolved zinc formed complexes with DOM in BR water compared to about 39% in ER water (Table S2); whereas the rest formed labile complexes that could also account for the observed toxicity as similarly reported elsewhere.[75]

The γ-nFe_2O_3 showed no cell membrane integrity effects to *B. subtilis* irrespective of water samples source across all exposure concentrations (Fig. 2b), and the results are in agreement with literature where no effects were observed on bacteria at concentrations of < 70 mgL^{-1} (< 70 000 μg L^{-1}). [52, 76, 77] In this study, no cytotoxic effects of γ-nFe_2O_3 were observed due to high aggregation (Table S1) that, in turn, reduced bacterial cell-nanoparticle contact. High aggregation was evident at higher exposure concentrations where γ-nFe_2O_3 sedimented to the bottom of the exposure vessels. And, due to γ-nFe_2O_3 low solubility, implied very low or,

non-release of ions especially in the short 2 h exposure period used in this study; further accounts why no cytotoxic effects were evident.

Herein, TEM was used to observe bacteria-ENPs interactions and the likely resultant effects on the bacterial cells, and the micrographs are shown in Fig. 3. For the γ-nFe_2O_3, intact bacteria cells at all nominal exposure concentrations (10–10 000 μg L^{-1}) were observed with only limited contact between the ENPs and cells as the exposure concentration increased (Fig. 3 (a-d)). Raptured cells were observed at higher concentrations of 100 and 1 000 μg L^{-1} for nZnO (Fig. 3 f and g), but the cells remained apparently intact at the lower concentration of 10 μg L^{-1}.

The cross-sections of *B. subtilis* following exposure to ENPs (Fig. 4) depicts a qualitative assessment on the integrity of membrane structures. At lower concentrations of 10 and 100 μg L^{-1}, γ-nFe_2O_3 intact cells were evident (Fig. 4 a and b), however, at higher ones (1 000 and 10 000 μg L^{-1}) as shown in Fig. 4 c and d, impairment of cell walls and membrane were observed likely due to close proximity of ENPs to the cells enhanced by increased aggregation as concentration increased as well as likely entrapment of cells in the formed aggregates. For nZnO, raptured cells were observed at 1 000 μg L^{-1} (Fig. 4 g), but at 10 and 100 μg L^{-1} qualitatively higher proportions of unimpaired cells were observed (Fig. 4 e and f

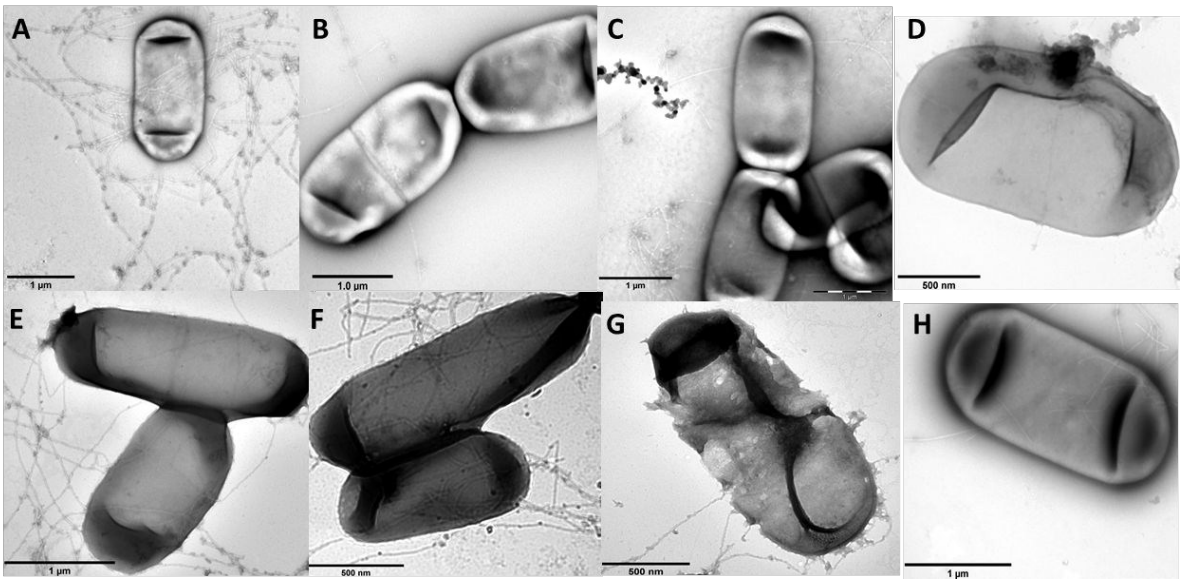

Fig. 3 Transmission electron micrographs of *B. subtilis* following exposure in (a) 10, (b) 100, (c) 1000, (d) 10000 μg L^{-1} γ-nFe_2O_3; (e) 10, (f) 100, (g) 1000 μg L^{-1} nZnO; and (h) control in ER.

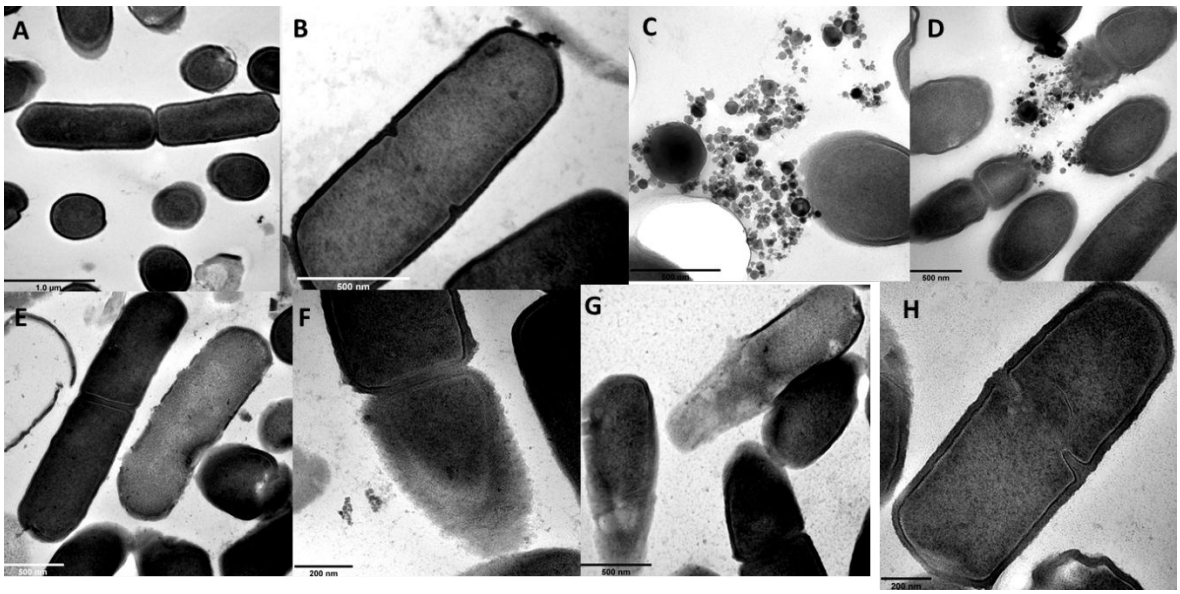

Fig. 4 Cross-sections of transmission electron micrographs of *B. subtilis* following exposure to (a) 10, (b) 100, (c) 1 000, (d) 10 000 μg L^{-1} γ-nFe_2O_3; (e) 10, (f) 100, (g) 1 000 μg L^{-1} nZnO; and (h) control in ER.

Bacterial cell wall serves as a barrier that controls and/or prevents the entry of certain compounds from the surrounding environment into the cell interior.[78, 79] Engineered nanoparticles have been reported to show anti-microbial activity through ENPs-induced disruption of the membrane.[10, 71, 80] Contact between the ENPs and bacteria, for example, where nZnO have been observed to cause cell wall permeability on *B. subtilis* was reported by Rago[54] and on other organisms.[22, 71] Herein, TEM results point to restricted contact between ENPs (nZnO and γ-nFe_2O_3) and bacteria cells with no evidence of uptake; yet cell membrane damage was observed in the case of nZnO. From our findings, negatively charged ENPs (as reported herein for both river water samples, Table S2) suggest minimal ENP-cell interactions (if any) due to repulsion, however, ENP-cell surface contact could not be ruled-out especially at higher concentrations where membrane damage occurred for nZnO. For instance, nZnO with HDD of 558 ± 28 nm as measured by DLS represents the average size of larger-sized particles; however, smaller-sized particles can still interact with

the bacteria cells due to the concentration effect as suggested by other researchers[81]. Such nZnO - bacteria interactions could also occur aided by mechanisms such as hydrogen bonding, Van der Waals forces, and receptor-ligand interactions through bacterial cell moieties where there's weak electrostatic repulsion.[74, 82, 83] However, no such similar effects were observed for γ-nFe_2O_3 due to formation of larger aggregates (μm sized) that tended to sediment and settle at the bottom of the vessels; thus leading to no plausible ENPs-cell interactions. Zn^{2+} have also been suggested to attach to the cell membrane and rupture the cell wall leading to membrane integrity loss.[84, 85] . In addition , in circumstances where disruption of zinc homeostasis occurs due to internalised Zn^{2+} cell death may occur through the denaturation of protein.[85-87] Tong et al,[44] for example, reported marked inhibition of between 10 and 20% on *Aeromonas hydrophila* and *E. coli* by nZnO (1 000 μg L^{-1}) under dark and light conditions without increased ROS production and with minimal contact between nZnO and bacterial cells. Therefore, results herein show Zn^{2+} effects may be via reduction of cellular functioning due to pure chemical effect in the bacterial cells.

ATP Production

In this study, the ability of ENPs to disrupt ATP production was also evaluated. Results of measured ATP abundance following exposure to nZnO and γ-nFe_2O_3 on *B. subtilis* in both water samples for 1 h are summarised in Fig. 5. ATP levels were observed to decline as a function of time, nominal exposure concentration, and water chemistry (Fig. 5). For example, nZnO exhibited significant concentration-dependent effects on ATP levels which were more pronounced in ER compared to BR water samples (Fig. 5a). To date, only limited studies have investigated the likely effects of ENPs on bacterial ATP levels[42-44]. Tong et al,[44] for example, reported significant concentration-dependent reduction in ATP levels exerted on *E.coli* and *A. hydrophila* by nZnO in lake water at concentrations of 250 and 1 000 μg L^{-1} following 1 h incubation under dark conditions.

Herein, our results revealed significant reduction on ATP levels even at lower concentration of 10 μg L^{-1} nZnO ($p < 0.05$) following 1 h incubation in river water under visible light. To account for these findings, we propose two plausible mechanisms. First, the depletion of cellular ATP may have been due to the disruption of cellular membrane leading to the loss of homeostasis in cells.[54, 87] Secondly, release of ions following the dissolution of ENPs (in

this case nZnO into dissolved zinc species) may have deactivated energy-dependent reactions in the cells as previously observed in toxicity studies of silver and zinc.[88, 89] In most organisms, Zn is an essential micronutrient required for biochemical processes, however; when present at elevated quantities may also interfere with biological pathways.[89] Therefore, the dissolved zinc from nZnO may have been taken up via the transport chains without causing damage to the cell membrane – but rather induced denaturation of ribosome and suppression of enzymes and proteins involved in ATP production – leading to the disruption of the cell functionality.[90, 91] This is consistent with the findings of nZnO toxicity in this study as evidenced by reduction in cell viability (Fig. 1a), and cell membrane integrity (Fig. 2a). This correlation is highly plausible due to two reasons. First, because minimal ENPs-cell contact was established, thus indicated unlikely cell membrane perforations (Fig. 3 e - g). And secondly, results herein indicate that the observed reduction in ATP levels followed the dissolution patterns responsible for the release of dissolved zinc as also earlier suggested by Tong et al.[44] Therefore, the observed variant nZnO effects between water matrixes from different sources were linked to differences in dissolution as influenced by water chemistry characteristics.

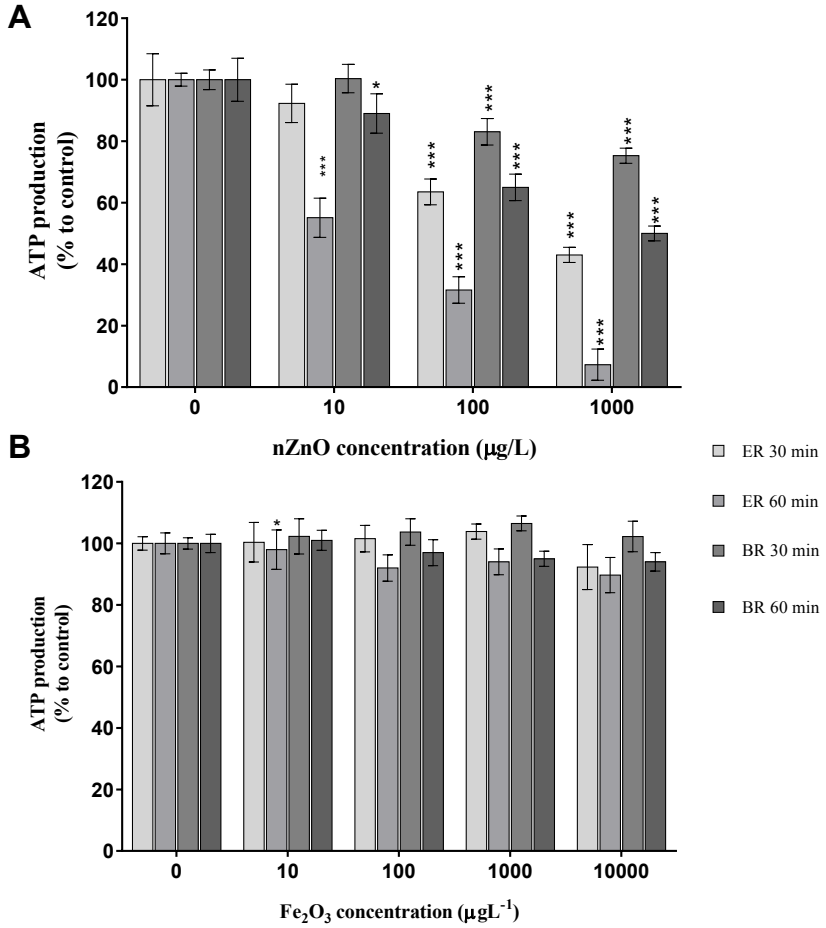

Fig. 5 Effects of (a) nZnO and (b) γ-nFe_2O_3 on *B. subtilis* ATP levels in ER and BR water samples. Percentage of bacterial ATP was normalized to that of the control (no exposure to ENPs). Asterisks (*) represent significance levels from Tukey's *post hoc* tests in two-way ANOVA (*$p < 0.05$, **$p \leq 0.01$, ***$p \leq 0.001$).

Results summarized in Fig. 5 also illustrates the influence of ENPs type on ATP production. The results in Fig. 5b show ATP levels following exposure to γ-nFe_2O_3 (compared to nZnO in Fig 5a) were insignificant irrespective of nominal exposure concentration and water chemistry in both water samples. In certain cases, however, like in BR γ-nFe_2O_3 was observed to induce increased ATP production levels above the control after 30 min incubation (Fig. 5b). To the authors' knowledge, this is for the first time ATP levels on bacteria exposed to γ-nFe_2O_3 in natural water samples were observed (10–10 000 μg L^{-1}). The lack of significant effects observed by ATP measurements, even at 10 000 μg L^{-1}, suggest that

γ-nFe_2O_3 may not pose any undesirable effect on microorganisms in aquatic systems, particularly at current predicted environmental concentrations of 28 ng L^{-1}.[92]

ROS production

To determine whether oxidative stress contributed to the observed effects of ENPs, ROS production was evaluated. Results showed that nZnO and nFe_2O_3 induced no significant change in intracellular ROS levels on *B. subtilis*, compared to the control, in both water samples under visible light conditions (Fig 6). Hence, these findings indicate that ROS production and oxidative stress were not linked to the observed nZnO toxicity.

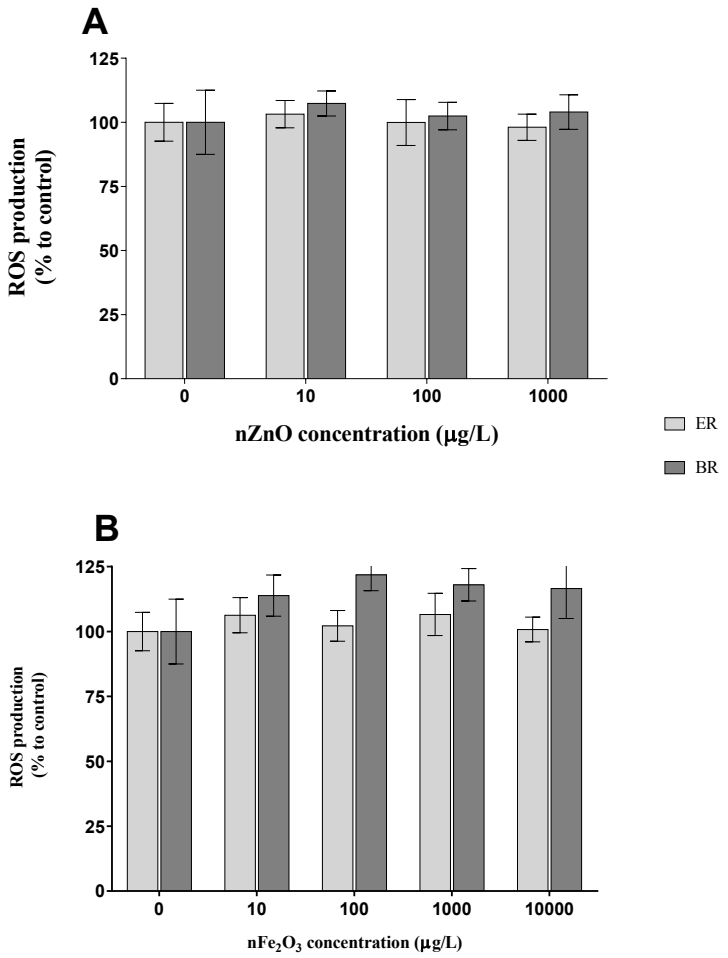

Fig. 6 Effects of (a) nZnO and (b) nFe_2O_3 on ROS levels in BR and ER water samples. Data represents the average ± SD (n=3). Asterisks (*) represent significance levels from Tukey's *post hoc* tests in two-way ANOVA (*$p < 0.05$, **$p \leq 0.01$, ***≤ 0.001).

To date, numerous studies have reported cell damage due to oxidative stress to be among the key toxicity causing mechanisms for metal-based ENPs.[25, 74, 93-95] For example, nZnO has been observed to induce significant ROS generation from *E. coli* relative to the control even in absence of UV illumination[71] – although at higher concentration of 8 mg L^{-1} (80 000 μg L^{-1}) but unlikely to be found in actual freshwater systems. Dasari and Hwang[32] observed cytotoxic effects in natural river water following exposure of nZnO to bacterial assemblages at 100 and 1 000 μg L^{-1} under both dark and light (sunlight) conditions, however; ROS generation was similar to the controls. Similarly, findings of Rago *et al*[54] revealed no induction of oxidative stress (ROS production) to *B. subtilis* following exposure to nZnO (10 – 250 000 μg L^{-1}); yet cytotoxic effects were observed.

Herein, results show that nZnO induced cytotoxicity and cell membrane damage to *B. subtilis* in both river water samples; but the observed effects could not be accounted for by ROS production (as it was absent). In addition, our results are consistent with observations of Dasari et al[32] where cytotoxicity was evident but could not be linked to oxidative stress. As argued by Kadiyala et al[83], and the evidence of results from this study, on cytotoxicity and cell membrane damage to *B. subtilis* indicate that ROS generation cannot be the predominant mechanism to account for the nZnO antimicrobial activity[87]. Therefore, more analysis is essential to elucidate the likely oxidative stress implications on the toxicity of ENPs, and particularly generate knowledge that can offer valuable insights that can account for the current contradictory data.

Environmental implications

The need to generate ENPs toxicity data from an environmental point of view, especially to build an understanding on their impacts to bacteria – organisms known to play a key role in efficient and effective functioning of the ecological systems – remain of high importance. This is because adverse effects to bacteria due to ENPs can trigger far reaching yet undesirable implications. To contribute towards achieving this objective, in this study, multiple lines of evidence on effects (lethal and sub-lethal) of ENPs to bacteria were considered – particularly at relevant likely exposure concentrations and in complex dynamic natural water matrices (sourced from two rivers). Evidence shows that differences in water

chemistry properties play a significant role on the observed (or lack thereof) effects of ENPs to microorganisms as they control the extent of ENPs bioavailability and transformation(s) in a given media. This means, based on the results generated from this study, it is not possible to generalize the effects of ENPs in freshwater, (whether at organism or sub-lethal level); rather the role of the water chemistry should be carefully considered.

To date, very limited studies have investigated the implications of ENPs to microorganisms in actual environmental matrices at relevant exposure concentrations such as freshwater used in this study. To contribute and improve risk assessment of ENPs in the environment, data presented herein particularly at sub-lethal level effects (cell membrane integrity and ATP production) should be considered even when no evidence of effects at whole body organisms, or even in absentia of widely known mechanisms of toxicity such as ROS production. This is because, exclusion of non-standard toxicity endpoints can lead to flawed conclusions if only absence of adverse effects of ENPs to microorganisms (based on effect or lethal concentration endpoints) are exclusively considered, and especially given the increasing concentrations of these emerging contaminants in different environmental compartments. The authors acknowledge that due to divergent and fragmented data especially on the mechanisms of toxicity and levels of toxicity on bacteria compounds the ability to make meaningful conclusions concerning the extent of ENPs implications to the environment. Thus, this points to two priority areas that needs urgent consideration – if risk assessment of ENPs in the environment particularly to microorganisms is to achieve a certain degree of standardization among experts in different fields (technical, regulatory and policy) similar to what has been done for their counterpart bulk chemicals.

Overall, the study findings suggest that γ-nFe_2O_3 at current environmental concentrations may not pose a risk to environmental organisms such as bacteria based on both physiological and sub-lethal effects. In contrast, the effects of nZnO on bacteria were dependent on the type of water chemistry where dissolution was a key precursor parameter to the observed toxicity. These results suggest that sub-cellular effects need to be incorporated jointly with traditional endpoints to establish the toxicity of ENPs, as the case with nZnO in this study vividly illustrates. However, findings herein cannot be deemed representative of all possible permutations of environmental conditions which could not be

considered in a single study. This raises the need to broaden testing conditions (represented by different sources of freshwater) including aspects such as irradiation and use of sensitive trophic levels e.g. crustaceans in natural water matrices. More data generated using natural waters as exposure media and in consideration of multiple toxicity endpoints will improve the possibility to undertake meaningful ecological risks of ENPs. Such approach will aid to draw firm conclusions necessary to map out proactive approaches aimed to manage nanoscale contaminants in a responsible and sustainable manner.

Conclusions

In this study, the toxicity of nZnO and γ-nFe_2O_3 in natural water samples with varying physicochemical parameters were assed. Results indicated that cell viability, cell membrane integrity, and ATP production were more diminished in ER (lower NOM, low IS, etc.) compared to BR (high NOM, high IS, etc.) water samples for nZnO exposures. However, γ-nFe_2O_3 induced very low or no cytotoxicity to microorganisms at exposure concentrations investigated in this work. In addition, we demonstrated that the toxicity of ENPs to *B. subtilis* were dependent chiefly on the differences in IS and NOM in the studied water samples. ROS production was observed to be negligible for both ENPs. Moreover, with no observed interactions of nZnO and bacteria indicated that the effects of nZnO were likely driven by dissolved zinc, and water chemistry played a key role as evidenced by the differences in their dissolution between the two water samples.

The study also illustrates the benefit of using multiple endpoints to assess the toxicity of ENPs as valuable insights on discrete effects were gained as certain endpoints showed no apparent responses but other revealed likely deleterious effects. For instance, in certain cases cell viability could not reveal cytotoxic effects of nZnO whereas cell membrane damage and ATP production demonstrated the effects of ENPs on bacteria. These findings suggest a plausible correlation between dissolved zinc and observed effects at different concentrations in the two water sources. This implies, the induced adverse interference on the metabolic pathways and cell membrane structures; which in turn, lead to the observed outcomes on bacteria, however, the nanoparticulate effects cannot be ruled out. Overall, the study

highlighted the complexity and variations in natural water sample physicochemical properties that should be considered when establishing the toxicity of ENPs to bacteria.

Conflicts of interest

There are no conflicts to declare.

Acknowledgements

This work was funded by the University of Pretoria (UP) (Grant No.: A0Y229), and the Water Research Commission (WRC) (K5/2509/1), South Africa. The contents are the sole responsibility of the authors and do not necessarily reflect the views of UP or the WRC. The authors would like to thank the Centre for Microbial Ecology and Genomics (CMEG) for use of their facilities and equipment; the Laboratory for Microscopy and Microanalysis at University of Pretoria for assistance with microscopy sample preparation and analysis, and Botswana International University of Science and Technology (BIUST) for use of their equipment. And, the comments and suggestions of three anonymous reviews are highly acknowledged since they aided to improve the quality of the manuscript.

References

1. F. Gottschalk, T. Sun and B. Nowack, Environmental concentrations of engineered nanomaterials: Review of modeling and analytical studies, *Environ. Pollut.*, 2013, **181**, 287-300.

2. S. F. Hansen, L. R. Heggelund, P. R. Besora, A. Mackevica, A. Boldrin and A. Baun, Nanoproducts–what is actually available to European consumers?, *Environ. Sci. Nano* 2016, **3**, 169-180.

3. Project on Emerging Nanotechnologies (PEN), Consumer Products Inventory: An inventory of nanotechnology-based consumer products introduced on the market, Available at. http://www.nanotechproject.org 2018).

4. The Nanodatabase, Jointly Published by: DTU Environment, the Danish Ecological Council and Danish Consumer Council., www.nanodb.dk, 2016).

5. K. Hegde, S. K. Brar, M. Verma and R. Y. Surampalli, Current understandings of toxicity, risks and regulations of engineered nanoparticles with respect to environmental microorganisms, *Nanotechnol. Environ. Eng.*, 2016, **1**, 5.

6. F. Gottschalk, C. Lassen, J. Kjoelholt, F. Christensen and B. Nowack, Modeling flows and concentrations of nine engineered nanomaterials in the Danish environment, *Int. J. Environ. Res. Public Health*, 2015, **12**, 5581-5602.

7. R. W. Lai, K. W. Yeung, M. M. Yung, A. B. Djurišić, J. P. Giesy and K. M. Leung, Regulation of engineered nanomaterials: current challenges, insights and future directions, *Environ. Sci. Pollut. Res.*, 2018, **25**, 3060-3077.

8. Ricardo Energy and Environment, *Support for 3rd regulatory review on nanomaterials-environmental legislation: Interim/Background Report.*, 2016.

9. J. W. Wiechers and N. Musee, Engineered inorganic nanoparticles and cosmetics: facts, issues, knowledge gaps and challenges, *J. Biomed. Nanotechnol.*, 2010, **6**, 408-431.

10. J. Hou, Y. Wu, X. Li, B. Wei, S. Li and X. Wang, Toxic effects of different types of zinc oxide nanoparticles on algae, plants, invertebrates, vertebrates and microorganisms, *Chemosphere*, 2018, **193**, 852-860.

11. D. L. Huber, Synthesis, properties, and applications of iron nanoparticles, *Small*, 2005, **1**, 482-501.

12. E. Demangeat, M. Pedrot, A. Dia, M. Bouhnik-Le-Coz, F. Grasset, K. Hanna, M. Kamagate and F. Cabello-Hurtado, Colloidal and chemical stabilities of iron oxide nanoparticles in aqueous solutions: the interplay of structural, chemical and environmental drivers, *Environ Sci. Nano* 2018, **5**, 992-1001.

13. Y. Zhang, B. Wu, H. Xu, H. Liu, M. Wang, Y. He and B. Pan, Nanomaterials-enabled water and wastewater treatment, *NanoImpact*, 2016, **3**, 22-39.

14. S. Rajput, L. P. Singh, C. U. Pittman Jr and D. Mohan, Lead (Pb^{2+}) and copper (Cu^{2+}) remediation from water using superparamagnetic maghemite (γ-Fe_2O_3) nanoparticles synthesized by Flame Spray Pyrolysis (FSP), *J. Colloid Interface Sci.*, 2017, **492**, 176-190.

15. C. Lei, L. Zhang, K. Yang, L. Zhu and D. Lin, Toxicity of iron-based nanoparticles to green algae: Effects of particle size, crystal phase, oxidation state and environmental aging, *Environ. Pollut.*, 2016, **218**, 505-512.

16. N. Musee, A model for screening and prioritizing consumer nanoproduct risks: A case study from South Africa, *Environ. Int.*, 2017, **100**, 121-131.

17. Y. Wang and B. Nowack, Environmental Risk Assessment of Engineered Nano-SiO_2, Nano Iron Oxides, Nano-CeO_2, Nano-Al_2O_3, and Quantum Dots, *Environ. Toxicol. Chem.*, 2018, **37**, 1387–1395.

18. F. Gottschalk, C. Ort, R. W. Scholz and B. Nowack, Engineered nanomaterials in rivers–exposure scenarios for Switzerland at high spatial and temporal resolution, *Environ. Pollut.*, 2011, **159**, 3439-3445.

19. T. Y. Sun, F. Gottschalk, K. Hungerbühler and B. Nowack, Comprehensive probabilistic modelling of environmental emissions of engineered nanomaterials, *Environ. Pollut.*, 2014, **185**, 69-76.

20. E. Dumont, A. C. Johnson, V. D. Keller and R. J. Williams, Nano silver and nano zinc-oxide in surface waters–Exposure estimation for Europe at high spatial and temporal resolution, *Environ. Pollut.*, 2015, **196**, 341-349.

21. N. Musee, M. Thwala and N. Nota, The antibacterial effects of engineered nanomaterials: implications for wastewater treatment plants, *J. Environ. Monit.*, 2011, **13**, 1164-1183.

22. S. Bandyopadhyay, G. Plascencia-Villa, A. Mukherjee, C. M. Rico, M. José-Yacamán, J. R. Peralta-Videa and J. L. Gardea-Torresdey, Comparative phytotoxicity of ZnO NPs, bulk ZnO, and ionic zinc onto the alfalfa plants symbiotically associated with *Sinorhizobium meliloti* in soil, *Sci. Total Environ.*, 2015, **515**, 60-69.

23. T. Qiu, J. Bozich, S. Lohse, A. Vartanian, L. Jacob, B. Meyer, I. Gunsolus, N. Niemuth, C. Murphy and C. Haynes, Gene expression as an indicator of the molecular response and toxicity in the bacterium Shewanella oneidensis and the water flea Daphnia magna exposed to functionalized gold nanoparticles, *Environ. Sci. Nano* 2015, **2**, 615-629.

24. A. Ivask, K. Juganson, O. Bondarenko, M. Mortimer, V. Aruoja, K. Kasemets, I. Blinova, M. Heinlaan, V. Slaveykova and A. Kahru, Mechanisms of toxic action of Ag, ZnO and CuO nanoparticles to selected ecotoxicological test organisms and mammalian cells in vitro: a comparative review, *Nanotoxicology*, 2014, **8**, 57-71.

25. C. Peng, W. Zhang, H. Gao, Y. Li, X. Tong, K. Li, X. Zhu, Y. Wang and Y. Chen, Behavior and potential impacts of metal-based engineered nanoparticles in aquatic environments, *Nanomaterials*, 2017, **7**, 21.

26. M. Zhu, H. Wang, A. A. Keller, T. Wang and F. Li, The effect of humic acid on the aggregation of titanium dioxide nanoparticles under different pH and ionic strengths, *Sci. Total Environ.*, 2014, **487**, 375-380.

27. C. Ren, X. Hu and Q. Zhou, Influence of environmental factors on nanotoxicity and knowledge gaps thereof, *NanoImpact*, 2016, **2**, 82-92.

28. J. Yi and J. Cheng, Effects of water chemistry and surface contact on the toxicity of silver nanoparticles to Bacillus subtilis, *Ecotoxicology*, 2017, **26**, 639-647.

29. S. M. Majedi, B. C. Kelly and H. K. Lee, Role of combinatorial environmental factors in the behavior and fate of ZnO nanoparticles in aqueous systems: a multiparametric analysis, *J. Hazard. Mater.*, 2014, **264**, 370-379.

30. Z. Wang, L. Zhang, J. Zhao and B. Xing, Environmental processes and toxicity of metallic nanoparticles in aquatic systems as affected by natural organic matter, *Environ. Sci. Nano* 2016, **3**, 240-255.

31. M. Li, D. Lin and L. Zhu, Effects of water chemistry on the dissolution of ZnO nanoparticles and their toxicity to *Escherichia coli*, *Environ. Pollut.*, 2012, **173**, 97-102.

32. T. P. Dasari and H.-M. Hwang, Effect of humic acids and sunlight on the cytotoxicity of engineered zinc oxide and titanium dioxide nanoparticles to a river bacterial assemblage, *J. Environ Sci.* , 2013, **25**, 1925–1935.

33. M. Heinlaan, M. Muna, M. Knöbel, D. Kistler, N. Odzak, D. Kühnel, J. Müller, G. S. Gupta, A. Kumar and R. Shanker, Natural water as the test medium for Ag and CuO nanoparticle hazard evaluation: an interlaboratory case study, *Environ. Pollut.*, 2016, **216**, 689-699.

34. M. Thwala, S. J. Klaine and N. Musee, Interactions of metal-based engineered nanoparticles with aquatic higher plants: A review of the state of current knowledge, *Environ. Toxicol. Chem.*, 2016, **35**, 1677-1694.

35. Y.-H. Peng, Y.-C. Tsai, C.-E. Hsiung, Y.-H. Lin and Y.-h. Shih, Influence of water chemistry on the environmental behaviors of commercial ZnO nanoparticles in various water and wastewater samples, *J. Hazard. Mater.*, 2017, **322**, 348-356.

36. N. Odzak, D. Kistler and L. Sigg, Influence of daylight on the fate of silver and zinc oxide nanoparticles in natural aquatic environments, *Environ. Pollut.*, 2017, **226**, 1-11.

37. J. R. Conway, A. S. Adeleye, J. Gardea-Torresdey and A. A. Keller, Aggregation, dissolution, and transformation of copper nanoparticles in natural waters, *Environ. Sci. Technol.*, 2015, **49**, 2749-2756.

38. C. T. T. Binh, T. Tong, J.-F. o. Gaillard, K. A. Gray and J. J. Kelly, Common freshwater bacteria vary in their responses to short-term exposure to nano-TiO_2, *Environ. Toxicol. Chem.*, 2014, **33**, 317–332.

39. P. A. Holden, J. L. Gardea-Torresdey, F. Klaessig, R. F. Turco, M. Mortimer, K. Hund-Rinke, E. A. Cohen Hubal, D. Avery, D. Barceló and R. Behra, Considerations of environmentally relevant test conditions for improved evaluation of ecological hazards of engineered nanomaterials, *Environ. Sci. Technol.*, 2016, **50**, 6124-6145.

40. C.-W. Huang, S.-W. Li and V. H.-C. Liao, Chronic ZnO-NPs exposure at environmentally relevant concentrations results in metabolic and locomotive toxicities in *Caenorhabditis elegans*, *Environ. Pollut.*, 2017, **220**, 1456-1464.

41. Z. Sheng and Y. Liu, Potential impacts of silver nanoparticles on bacteria in the aquatic environment, *J. Environ. Manage.*, 2017, **191**, 290-296.

42. C. M. Wilke, T. Tong, J.-F. o. Gaillard and K. A. Gray, Attenuation of Microbial Stress Due to Nano-Ag and Nano-TiO_2 Interactions under Dark Conditions, *Environ. Sci. Technol.*, 2016, **50**, 11302−11310.

43. C. M. Wilke, J.-F. Gaillard and K. A. Gray, The critical role of light in moderating microbial stress due to mixtures of engineered nanomaterials, *Environ. Sci. Nano* 2017.

44. T. Tong, C. M. Wilke, J. Wu, C. T. T. Binh, J. J. Kelly, J.-F. o. Gaillard and K. A. Gray, Combined Toxicity of Nano-ZnO and Nano-TiO_2: From Single- to Multinanomaterial Systems, *Environ. Sci. Technol.*, 2015, **49**, 8113−8123.

45. A. M. Earl, R. Losick and R. Kolter, Ecology and genomics of *Bacillus subtilis*, *Trends Microbiol.*, 2008, **16**, 269-275.

46. Y.-W. Baek and Y.-J. An, Microbial toxicity of metal oxide nanoparticles (CuO, NiO, ZnO, and Sb_2O_3) to *Escherichia coli*, *Bacillus subtilis*, and *Streptococcus aureus*, *Sci. Total Environ.*, 2011, **409**, 1603–1608.

47. C. Pagnout, S. Jomini, M. Dadhwal, C. Caillet, F. Thomas and P. Bauda, Role of electrostatic interactions in the toxicity of titanium dioxide nanoparticles toward *Escherichia coli*, *Colloids Surf. B*, 2012, **92**, 315-321.

48. A. Hitchman, G. H. S. Smith, Y. Ju-Nam, M. Sterling and J. R. Lead, The effect of environmentally relevant conditions on PVP stabilised gold nanoparticles, *Chemosphere*, 2013, **90**, 410-416.

49. T. M. Riddick, Control of colloid stability through zeta potential, *Blood*, 1968, **10**.

50. R. W. O'Brien and L. R. White, Electrophoretic mobility of a spherical colloidal particle, *J. Chem. Soc., Faraday Trans. 2*, 1978, **74**, 1607-1626.

51. G. V. Lowry, R. J. Hill, S. Harper, A. F. Rawle, C. O. Hendren, F. Klaessig, U. Nobbmann, P. Sayre and J. Rumble, Guidance to improve the scientific value of zeta-potential measurements in nanoEHS, *Environ. Sci. Nano* 2016, **3**, 953-965.

52. D. Wang, Z. Lin, T. Wang, Z. Yao, M. Qin, S. Zheng and W. Lu, Where does the toxicity of metal oxide nanoparticles come from: the nanoparticles, the ions, or a combination of both?, *J. Hazard. Mater.*, 2016, **308**, 328-334.

53. M. Li, S. Pokhrel, X. Jin, L. Mädler, R. Damoiseaux and E. M. Hoek, Stability, bioavailability, and bacterial toxicity of ZnO and iron-doped ZnO nanoparticles in aquatic media, *Environ. Sci. Technol.*, 2010, **45**, 755-761.

54. I. Rago, C. R. Chandraiahgari, M. P. Bracciale, G. De Bellis, E. Zanni, M. C. Guidi, D. Sali, A. Broggi, C. Palleschi and M. S. Sarto, Zinc oxide microrods and nanorods: different antibacterial activity and their mode of action against Gram-positive bacteria, *RSC Adv.*, 2014, **4**, 56031-56040.

55. N. Musee, J. N. Zvimba, L. M. Schaefer, N. Nota, L. M. Sikhwivhilu and M. Thwala, Fate and behavior of ZnO-and Ag-engineered nanoparticles and a bacterial viability assessment in a simulated wastewater treatment plant, *J. Environ. Sci. Health A*, 2014, **49**, 59-66.

56. M. Baalousha, A. Manciulea, S. Cumberland, K. Kendall and J. R. Lead, Aggregation and surface properties of iron oxide nanoparticles: influence of pH and natural organic matter, *Environ. Toxicol. Chem.* , 2008, **27**, 1875-1882.

57. R. Khan, M. Inam, S. Zam, D. Park and I. Yeom, Assessment of key environmental factors influencing the sedimentation and aggregation behavior of zinc oxide nanoparticles in aquatic environment, *Water*, 2018, **10**, 660.

58. S. Yu, J. Liu, Y. Yin and M. Shen, Interactions between engineered nanoparticles and dissolved organic matter: A review on mechanisms and environmental effects, *J. Environ. Sci.* , 2018, **63**, 198-217.

59. A. Philippe and G. E. Schaumann, Interactions of dissolved organic matter with natural and engineered inorganic colloids: a review, *Environ. Sci. Technol.*, 2014, **48**, 8946-8962.

60. B. Collin, M. Auffan, A. C. Johnson, I. Kaur, A. A. Keller, A. Lazareva, J. R. Lead, X. Ma, R. C. Merrifield and C. Svendsen, Environmental release, fate and ecotoxicological effects of manufactured ceria nanomaterials, *Environ Sci. Nano* 2014, **1**, 533-548.

61. A. Nebbioso and A. Piccolo, Molecular characterization of dissolved organic matter (DOM): a critical review, *Anal. Bioanal. Chem.*, 2013, **405**, 109-124.

62. S. M. Louie, R. D. Tilton and G. V. Lowry, Critical review: impacts of macromolecular coatings on critical physicochemical processes controlling environmental fate of nanomaterials, *Environ. Sci. Nano* 2016, **3**, 283-310.

63. S.-W. Bian, I. A. Mudunkotuwa, T. Rupasinghe and V. H. Grassian, Aggregation and dissolution of 4 nm ZnO nanoparticles in aqueous environments: influence of pH, ionic strength, size, and adsorption of humic acid, *Langmuir*, 2011, **27**, 6059-6068.

64. A. J. Miao, X. Y. Zhang, Z. Luo, C. S. Chen, W. C. Chin, P. H. Santschi and A. Quigg, Zinc oxide–engineered nanoparticles: dissolution and toxicity to marine phytoplankton, *Environ. Toxicol. Chem.*, 2010, **29**, 2814-2822.

65. X. He, W. G. Aker, P. P. Fu and H.-M. Hwang, Toxicity of engineered metal oxide nanomaterials mediated by nano–bio–eco–interactions: a review and perspective, *Environ. Sci. Nano* 2015, **2**, 564-582.

66. D. Zhou and A. A. Keller, Role of morphology in the aggregation kinetics of ZnO nanoparticles, *Water Res.*, 2010, **44**, 2948-2956.

67. J. Fang, A. Shijirbaatar, D.-h. Lin, D.-j. Wang, B. Shen and Z.-q. Zhou, Stability of co-existing ZnO and TiO_2 nanomaterials in natural water: Aggregation and sedimentation mechanisms, *Chemosphere*, 2017, **184**, 1125-1133.

68. J. Lv, S. Zhang, L. Luo, W. Han, J. Zhang, K. Yang and P. Christie, Dissolution and microstructural transformation of ZnO nanoparticles under the influence of phosphate, *Environ. Sci. Technol.*, 2012, **46**, 7215-7221.

69. M. Heinlaan, A. Ivask, I. Blinova, H.-C. Dubourguier and A. Kahru, Toxicity of nanosized and bulk ZnO, CuO and TiO2 to bacteria Vibrio fischeri and crustaceans Daphnia magna and Thamnocephalus platyurus, *Chemosphere*, 2008, **71**, 1308-1316.

70. V. Aruoja, H. C. Dubourguier, K. Kasemets and A. Kahru, Toxicity of nanoparticles of CuO, ZnO and TiO2 to microalgae *Pseudokirchneriella subcapitata*, *Sci. Total Environ.*, 2009, **407**, 1461-1468.

71. A. Kumar, A. K. Pandey, S. S. Singh, R. Shanker and A. Dhawan, Engineered ZnO and TiO_2 nanoparticles induce oxidative stress and DNA damage leading to reduced viability of *Escherichia coli*, *Free Radic. Biol. Med.*, 2011, **51**, 1872-1881.

72. A. Jain, R. Bhargava and P. Poddar, Probing interaction of Gram-positive and Gram-negative bacterial cells with ZnO nanorods, *Mater. Sci. Eng. C*, 2013, **33**, 1247-1253.

73. Y. C. Huang, R. Fan, M. A. Grusak, J. D. Sherrier and C. Huang, Effects of nano-ZnO on the agronomically relevant Rhizobium–legume symbiosis, *Sci. Total Environ.*, 2014, **497**, 78-90.

74. Y. H. Leung, X. Xu, A. P. Ma, F. Liu, A. M. Ng, Z. Shen, L. A. Gethings, M. Y. Guo, A. B. Djurišić and P. K. Lee, Toxicity of ZnO and TiO_2 to *Escherichia coli* cells, *Sci. Rep.*, 2016, **6**, 35243.

75. M. Li, L. Zhu and D. Lin, Toxicity of ZnO nanoparticles to *Escherichia coli*: mechanism and the influence of medium components, *Environ. Sci. Technol.*, 2011, **45**, 1977-1983.

76. M. Auffan, W. Achouak, J. Rose, M.-A. Roncato, C. Chanéac, D. T. Waite, A. Masion, J. C. Woicik, M. R. Wiesner and J.-Y. Bottero, Relation between the redox state of iron-based nanoparticles and their cytotoxicity toward *Escherichia coli*, *Environ. Sci. Technol.*, 2008, **42**, 6730-6735.

77. A. Azam, A. S. Ahmed, M. Oves, M. S. Khan, S. S. Habib and A. Memic, Antimicrobial activity of metal oxide nanoparticles against Gram-positive and Gram-negative bacteria: a comparative study, *Int. J. Nanomed.*, 2012, **7**, 6003–6009.

78. W. Dowhan and M. Bogdanov, in *New comprehensive biochemistry*, Elsevier, 2002, vol. 36, pp. 1-35.

79. S. Murínová and K. Dercová, Response mechanisms of bacterial degraders to environmental contaminants on the level of cell walls and cytoplasmic membrane, *Int. J. Microbiol.*, 2014, **2014**.

80. A. Sirelkhatim, S. Mahmud, A. Seeni, N. H. M. Kaus, L. C. Ann, S. K. M. Bakhori, H. Hasan and D. Mohamad, Review on zinc oxide nanoparticles: antibacterial activity and toxicity mechanism, *Nano-Micro Lett.*, 2015, **7**, 219-242.

81. D. Wang, Y. Gao, Z. Lin, Z. Yao and W. Zhang, The joint effects on Photobacterium phosphoreum of metal oxide nanoparticles and their most likely coexisting chemicals in the environment, *Aquat. Toxicol.*, 2014, **154**, 200-206.

82. W. Jiang, H. Mashayekhi and B. Xing, Bacterial toxicity comparison between nano- and micro-scaled oxide particles, *Environ. Pollut.*, 2009, **157**, 1619-1625.

83. U. Kadiyala, E. S. Turali-Emre, J. H. Bahng, N. A. Kotov and J. S. VanEpps, Unexpected insights into antibacterial activity of zinc oxide nanoparticles against methicillin resistant Staphylococcus aureus (MRSA), *Nanoscale*, 2018, **10**, 4927-4939.

84. J. A. Lemire, J. J. Harrison and R. J. Turner, Antimicrobial activity of metals: mechanisms, molecular targets and applications, *Nat. Rev. Microbiol.*, 2013, **11**, 371.

85. E. L. Yu-sen, R. D. Vidic, J. E. Stout, C. A. McCartney and L. Y. Victor, Inactivation of *Mycobacterium avium* by copper and silver ions, *Water Res.*, 1998, **32**, 1997-2000.

86. C. B. Anders, J. E. Eixenberger, N. A. Franco, R. J. Hermann, K. D. Rainey, J. J. Chess, A. Punnoose and D. G. Wingett, ZnO nanoparticle preparation route influences surface reactivity, dissolution and cytotoxicity, *Environ. Sci. Nano.*, 2018, **5**, 572-588.

87. K. Matuła, Ł. Richter, W. Adamkiewicz, B. Åkerström, J. Paczesny and R. Hołyst, Influence of nanomechanical stress induced by ZnO nanoparticles of different shapes on the viability of cells, *Soft matter*, 2016, **12**, 4162-4169.

88. A. Lapresta-Fernández, A. Fernández and J. Blasco, Nanoecotoxicity effects of engineered silver and gold nanoparticles in aquatic organisms, *Trends Anal. Chem.*, 2012, **32**, 40-59.

89. A. Alhasawi, C. Auger, V. Appanna, M. Chahma and V. Appanna, Zinc toxicity and ATP production in *Pseudomonas fluorescens*, *J. Appl. Microbiol.*, 2014, **117**, 65-73.

90. C. Krishnaraj, E. Jagan, S. Rajasekar, P. Selvakumar, P. Kalaichelvan and N. Mohan, Synthesis of silver nanoparticles using Acalypha indica leaf extracts and its antibacterial activity against water borne pathogens, *Colloids Surf. B*, 2010, **76**, 50-56.

91. M. Yamanaka, K. Hara and J. Kudo, Bactericidal actions of a silver ion solution on *Escherichia coli*, studied by energy-filtering transmission electron microscopy and proteomic analysis, *Appl. Environ. Microbiol.*, 2005, **71**, 7589-7593.

92. Y. Wang, L. Deng, A. Caballero-Guzman and B. Nowack, Are engineered nano iron oxide particles safe? An environmental risk assessment by probabilistic exposure, effects and risk modeling, *Nanotoxicology*, 2016, **10**, 1545-1554.

93. G. Vale, K. Mehennaoui, S. Cambier, G. Libralato, S. Jomini and R. F. Domingos, Manufactured nanoparticles in the aquatic environment-biochemical responses on freshwater organisms: a critical overview, *Aquat. Toxicol.*, 2016, **170**, 162-174.

94. N. von Moos and V. I. Slaveykova, Oxidative stress induced by inorganic nanoparticles in bacteria and aquatic microalgae–state of the art and knowledge gaps, *Nanotoxicology*, 2014, **8**, 605-630.

95. T. P. Dasari, K. Pathakoti and H.-M. Hwang, Determination of the mechanism of photoinduced toxicity of selected metal oxide nanoparticles (ZnO, CuO, Co_3O_4 and TiO_2) to *E. coli* bacteria, *J. Environ Sci.* , 2013, **25**, 882–888.